AIMS Mathematics, 10(11): 27816–27836.
DOI:10.3934/math.20251222
Received: 21 June 2025
Revised: 06 November 2025
Accepted: 18 November 2025
Published: 28 November 2025

https://www.aimspress.com/journal/Math

Research article

Neutrosophic moment exponential distribution: properties and modeling of child mortality rate data

Ghadah Alomani[1], R. Maya[2], M. R. Irshad[2], Amer I. Al-Omari[3,*] and A. S. Aparna[2]

[1] Department of Mathematical Sciences, College of Science, Princess Nourah bint Abdulrahman University, P.O. Box 84428, Riyadh 11671, Saudi Arabia

[2] Department of Statistics, Cochin University of Science and Technology, Cochin 682 022, Kerala, India

[3] Department of Mathematics, Faculty of Science, Al Al-Bayt University, Mafraq 25113, Jordan

* **Correspondence:** Email: alomari_amer@yahoo.com.

Abstract: This research extends traditional statistical distribution theory, which often neglects issues such as ambiguity, imprecision, or indeterminacy. The primary aim is to develop the neutrosophic moment exponential distribution as a refined version of the moment exponential distribution, specifically to tackle situations involving uncertainty. The study derives the proposed model's quantile function, Mills ratio, and elasticity, as well as its mean, variance, r^{th} moment, index of dispersion, and moment-generating function. It also establishes expressions for the survival function, hazard rate function, cumulative hazard function, and mean residual life function, which are visually explored through graphs. Furthermore, the research calculates information measures including extropy, weighted extropy, cumulative residual extropy, Shannon entropy, and Rényi entropy. The parameters of the proposed model are determined using maximum likelihood estimation, followed by a simulation study and an illustration of the distribution of the order statistics. Finally, the practical superiority of the proposed distribution over several existing models in the literature is demonstrated using a child mortality rate dataset.

Keywords: neutrosophic distribution; indeterminacy; survival function; hazard rate function; parameter estimation
Mathematics Subject Classification: 60E05, 62A86

1. Introduction

In the complex and uncertain real world, where situations are ambiguous and problems lack clarity, assigning specific values to statistical characteristics becomes challenging. Classical probability

distribution falls short in delivering accurate results in such imprecise scenarios. Developing new probability distributions is essential in statistical modeling and data analysis, as it enables researchers to more effectively represent real-world phenomena. Standard distributions may not always adequately describe complex data patterns, particularly in areas such as engineering, finance, and healthcare. By introducing new distributions, researchers enhance models' adaptability, improve predictive performance, and offer deeper insights into uncertainty and variability. Additionally, these innovations contribute to advancements in probability theory and provide valuable tools for informed decision-making under uncertainty. A lot of new distributions are suggested as modifications to some existing distributions, such as the new extended-X exponentiated inverted Weibull distribution proposed by [1]. Al-Omari et al. [2] suggested the unit two parameter Mirra distribution. These authors [3] also introduced asymmetric right-skewed size-biased Bilal distribution, and others [4] suggested the Marshall–Olkin Bilal distribution with investigation to acceptance sampling plans. Irshad et al. [5] proposed a versatile model designed for bounded data, featuring a bathtub-shaped hazard rate function (HRF). Recent advancements explore alternative approaches like fuzzy logic and neutrosophy to model these situations more effectively. Numerous studies have explored neutrosophic probability distributions to assess uncertainty in real-world problems, yielding more favorable outcomes compared with classical statistics.

Uncertainty modeling has garnered significant interest among scientists and engineers, as it enables the extraction and interpretation of valuable information from uncertain data. Smarandache [6] introduced neutrosophic statistics to handle uncertainties or unclear aspects within data and presented the concept of neutrosophic logic, using the components T, I, and F to signify truth, indeterminacy, and falsehood, respectively. Zeina and Hatip [7] developed neutrosophic random variables, analyzing the statistical properties and providing examples. Patro and Smarandache [8] introduced neutrosophic binomial and neutrosophic normal distributions. Alhabib et al. [9] explored neutrosophic statistics by developing neutrosophic probability distributions derived from classical distributions like Poisson, exponential, and uniform. Alhasan and Smarandache [10] examined the characteristics of the neutrosophic Weibull distribution. Alanzi et al. [11] offered a neutrosophic Poisson moment exponential distribution with applications. Sherwani et al. [12] proposed the neutrosophic beta distribution, exploring its properties and applications, while the authors of [13] introduced the neutrosophic gamma distribution. Additionally, [14] proposed the neutrosophic Rayleigh model for engineering applications, and [15] proposed a new neutrosophic model based on the Dinesh–Umesh–Sanjay (DUS)–Weibull transformation. Zeina et al. [16] studied the neutrosophic Kumaraswamy probability distribution. The neutrosophic quasi-XLindley distribution was suggested by [17]. Al-Essa et al. [18] suggested a neutrosophic Burr XII distribution and investigated its properties. These distributions provide a wider framework in the field, tackling issues that classical statistics often ignore because of indeterminacy.

In recent years, researchers have made significant contributions to the advancement of neutrosophic statistics, both methodologically and in practical applications. Alhabib and Salama [19] introduced time-series theory within the framework of indeterminacy, while the authors of [20] extended neutrosophic statistics to the field of total quality control by proposing control charts in indeterminate environments and developing several neutrosophic sampling plans.

In this paper, we considered the moment exponential distribution (MED), proposed by [21] as a base distribution, which enhances the conventional exponential distribution by incorporating weights

derived from Fisher's (1934) theory. The probability density function (PDF) of the MED is expressed with the scale parameter β as follows:

$$f(x;\beta) = \begin{cases} \frac{x}{\beta^2} e^{-\frac{x}{\beta}}, & \text{if } x > 0, \beta > 0, \\ 0, & \text{otherwise.} \end{cases} \tag{1.1}$$

The cumulative distribution function (CDF) is given by the following expression:

$$F(x;\beta) = 1 - \left(1 + \frac{x}{\beta}\right) e^{-\left(\frac{x}{\beta}\right)}, \quad \text{if } x > 0,\ \beta > 0. \tag{1.2}$$

The moment-generating function (MGF) and the r^{th} moment of the MED are defined as:

$$M_X(t) = (1 - \beta t)^{-2}, \quad \text{if } t \geq 0, \text{and} \quad \mu'_r = E(X^r) = \beta^r \Gamma(2 + r). \tag{1.3}$$

Figure 1 includes the MED's PDF plots for some values of the parameter. The plot reveals that the MED is asymmetric and positively skewed.

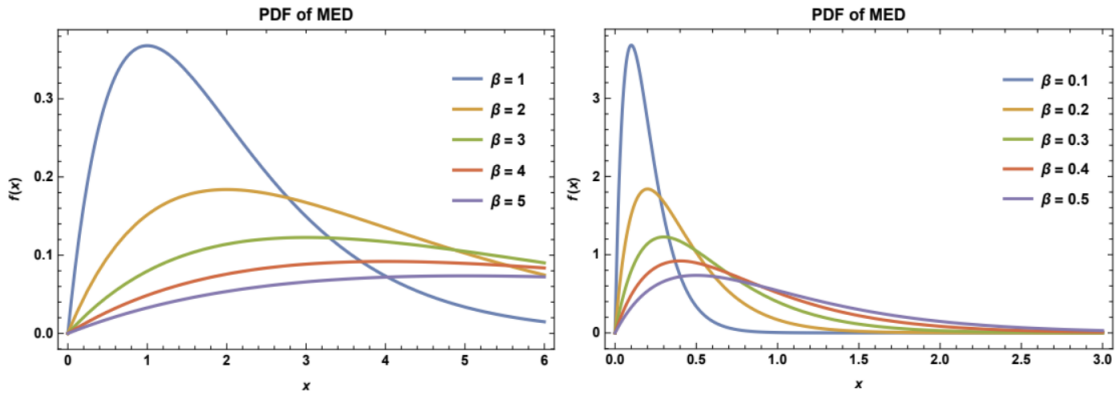

Figure 1. The MED PDF plots for some values of β.

For more about the MED, see [21]. The MED has gained significant attention for its versatility, leading various researchers to explore and extend it for handling more intricate datasets. Building on this, notable extensions include the exponentiated MED of [22], the Marshall–Olkin length-biased exponential distribution of [23], the Kumaraswamy MED of [24], the Poisson moment exponential distribution with associated regression and INAR(1) process of [25], and other related works. Despite these advances, there remains a need for more flexible generalizations capable of capturing uncertainty in real-world datasets. To address this gap, the present study introduces the neutrosophic moment exponential distribution (NMED), which incorporates the concept of indeterminacy into the classical moment exponential framework. While traditional models assume exact and precise data, many practical applications—such as survival analysis, economics, wealth modeling, and network data—are subject to ambiguity, measurement error, or incomplete information. The neutrosophic extension provides a robust approach for handling such uncertainty, making the NMED a flexible and powerful tool for analyzing lifetime data. The objectives of this study are the following.

(1) Develop the NMED as an extension of the MED to handle uncertainty, imprecision, and indeterminacy;

(2) Derive and analyze key statistical properties of the NMED, such as its mean, variance, r^{th} moment, index of dispersion, MGF, order statistics, quantile function, Shannon entropy, Rényi entropy, and survival function (SF);

(3) Estimate the parameters of the NMED using the maximum likelihood (ML) estimation method and validate its performance through a simulation study;

(4) Compare the practical efficacy of the NMED with the existing different distributions in the literature using real dataset.

The paper is structured as follows: Section 2 introduces the proposed NMED, including its CDF and PDF, and their graphical representations. Section 3 explores various statistical properties of the NMED, supported by their proofs. In Section 4, the Shannon and Rényi entropies are discussed. Parameter estimation is addressed in Section 5. A simulation study is conducted in Section 6. Section 7 provides applications using a real-world dataset. The paper concludes in Section 8.

2. The proposed NMED

In this section, we describe the NMED and elucidate some of its properties. Let $X_N = X + I$ be a neutrosophic random variable, where X is a classical random variable and I is an indeterminacy component. Suppose that the CDF of X is given by $F_X(x) = P(X \leq x)$. In this case, the CDF and PDF of the neutrosophic random variable X_N are given by

$$F(x_N) = F_X(x - I), \text{and } f(x_N) = f_X(x - I),$$

where $F(x_N)$ and $f(x_N)$ denote the CDF and PDF of the neutrosophic variable X_N, respectively [26]. Using the same idea, the PDF of the suggested NMED is given by

$$f(x_N;\beta) = \frac{(x_N - I)}{\beta^2} e^{-\frac{x_N - I}{\beta}}, \quad \text{if } I < x_N < \infty, \beta > 0. \tag{2.1}$$

It can be easily demonstrated that Eq (2.1) fulfills the requirements of being a PDF, where $f(x_N;\beta)$ is positive and

$$\begin{aligned}\int_I^\infty \frac{(x_N - I)}{\beta^2} e^{-\frac{x_N - I}{\beta}} \, dx_N &= \frac{1}{\beta^2}\left[\int_I^\infty x_N e^{-\frac{x - I}{\beta}} \, dx_N - I\int_I^\infty e^{-\frac{x_N - I}{\beta}} \, dx_N\right] \\ &= \frac{1}{\beta^2}[I\beta + \beta^2 - I\beta] \\ &= 1.\end{aligned}$$

To find the CDF $F(x_N)$ of the PDF defined in 2.1, we compute

$$\begin{aligned}F(x_N;\beta) = P(X_N \leq x_N) &= \int_I^{x_N} f(t;\beta)dt \\ &= \int_I^x \frac{(t - I)}{\beta^2} e^{-\frac{t - I}{\beta}} dt.\end{aligned}$$

We use the substitution

$$u = \frac{t - I}{\beta} \quad \Rightarrow \quad du = \frac{dt}{\beta} \quad \Rightarrow \quad dt = \beta du.$$

Simplifying, we have

$$F(x_N;\beta) = = \int_0^{\frac{x_N-I}{\beta}} \frac{\beta u}{\beta^2} e^{-u} \beta du$$
$$= \int_0^{\frac{x_N-I}{\beta}} ue^{-u} du = 1 - \left(\frac{x_N - I}{\beta} + 1\right) e^{-\frac{x_N-I}{\beta}}.$$

Thus, the CDF of the NMED is given by

$$F(x_N;\beta) = \begin{cases} 0, & x_N \leq I, \\ 1 - \left(\frac{x_N-I}{\beta} + 1\right) e^{-\frac{x_N-I}{\beta}}, & x_N > I. \end{cases} \tag{2.2}$$

Figure 2 displays the PDF and CDF plots for different combinations of the distribution parameter β and the indeterminacy factor I, specifically for the pairs $(\beta = 2, I = 1.55)$, $(\beta = 3, I = 1.55)$, $(\beta = 2, I = 2.59)$, $(\beta = 3, I = 2.59)$, $(\beta = 2, I = 3.54)$, $(\beta = 3, I = 3.54)$, $(\beta = 2, I = 4.91)$, and $(\beta = 3, I = 4.91)$. These plots highlight how changes in β and I affect the distribution's shape and behavior, showing right-skewed curves with increasing–decreasing patterns, which enhance the distribution's adaptability for modeling various data types.

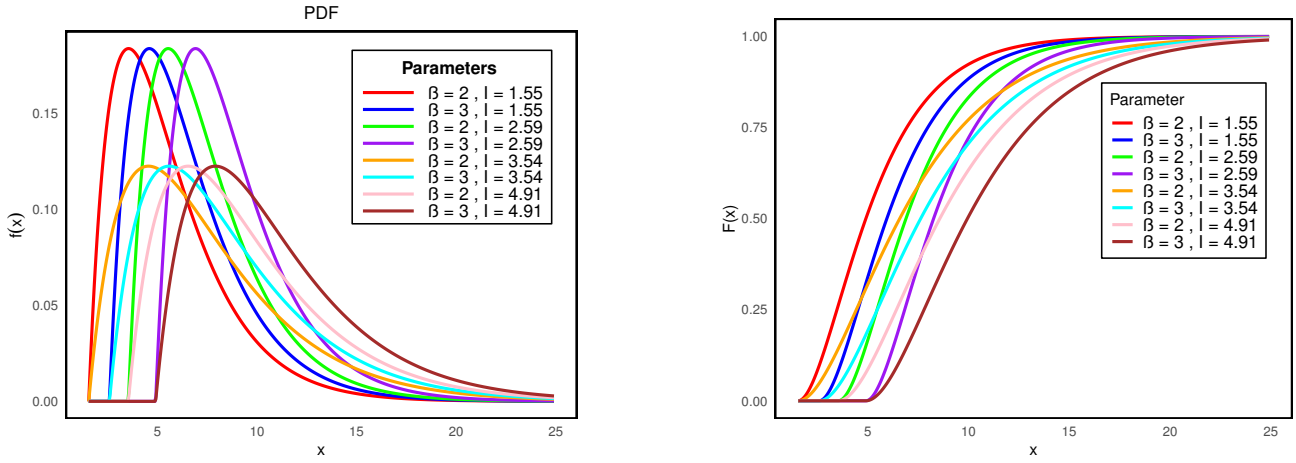

Figure 2. PDF and CDF plots of the NMED.

3. Statistical properties of the NMED

This section details several statistical characteristics of the NMED, such as the mean, variance, index of dispersion (IOD), MGF, r^{th} moment, SF, cumulative hazard function (CHF), HRF, mean residual life function (MRLF), as well as Shannon and Rényi entropies, extropy, weighted extropy, and cumulative residual extropy. These properties offer important insights into the distribution's behavior and its fundamental attributes.

3.1. The r^{th} moment

Theorem 1. The r^{th} moment of the NMED is given by

$$\mathbb{E}[X_N^r] = \sum_{k=0}^{r} \binom{r}{k} I^{r-k}(k+1)!\beta^k. \tag{3.1}$$

Proof. The proof starts by finding the expectation of X_N^r denoted as follows:

$$\begin{aligned}
\mathbb{E}[X_N^r] &= \int_I^\infty x_N^r \frac{(x_N - I)}{\beta^2} e^{-\frac{x_N - I}{\beta}}\, dx_N, \text{using } \; u = x_N - I, \text{and } \; du = dx_N \\
&= \int_0^\infty (u+I)^r \frac{u}{\beta^2} e^{-u/\beta}\, du \\
&= \sum_{k=0}^{r} \binom{r}{k} I^{r-k} \int_0^\infty u^{k+1} \frac{1}{\beta^2} e^{-u/\beta}\, du, \text{using } \; (u+I)^r = \sum_{k=0}^{r} \binom{r}{k} I^{r-k} u^k \\
&= \sum_{k=0}^{r} \binom{r}{k} I^{r-k} \frac{(k+1)!}{\beta^2} \beta^{k+2}, \int_0^\infty u^m e^{-u/\beta}\, du = \Gamma(m+1)\beta^{m+1} = m!\beta^{m+1} \\
&= \sum_{k=0}^{r} \binom{r}{k} I^{r-k}(k+1)!\beta^k, \int_0^\infty u^{k+1} e^{-u/\beta}\, du = (k+1)!\beta^{k+2}.
\end{aligned}$$

The first four moments of the NMED can be obtained by setting $r = 1, 2, 3, 4$ in Eq (3.1) as follows:

$$\mathbb{E}\left(X_N\right) = 2\beta + I,$$
$$\mathbb{E}\left(X_N^2\right) = I^2 + 4I\beta + 6\beta^2,$$

$$\mathbb{E}\left(X_N^3\right) = I^3 + 6I^2\beta + 18I\beta^2 + 24\beta^3,$$
$$\mathbb{E}\left(X_N^4\right) = I^4 + 8I^3\beta + 36I^2\beta^2 + 96I\beta^3 + 120\beta^4.$$

The variance of the NMED is given by

$$\mathbb{V}(X_N) = \mathbb{E}(X_N^2) - [\mathbb{E}(X_N)]^2 = 2\beta^2.$$

3.2. Index of dispersion

The IOD, calculated as the ratio of the variance to the mean, acts as a measure to determine the suitability of a distribution for datasets exhibiting under-dispersion or over-dispersion. For the NMED, the IOD is expressed as

$$IOD(X_N) = \frac{\mathbb{V}(X_N)}{\mathbb{E}(X_N)} = \frac{2\beta^2}{2\beta + I}. \tag{3.2}$$

3.3. Moment-generating function

The MGF provides a compact way to analyze the properties of random variables, including their moments, distributions, and behaviors under transformations, making it a powerful tool in probability theory and statistics.

Theorem 2. The MGF of the NMED is given by

$$M_{X_N}(t) = \frac{e^{tI}}{(1-\beta t)^2}, \quad \text{for } t < \frac{1}{\beta}. \tag{3.3}$$

Proof. To prove this theorem, the MGF of a random variable X_N is defined as

$$\begin{aligned} M_{X_N}(t) &= \int_I^\infty e^{tx_N} \frac{(x_N - I)}{\beta^2} e^{-\frac{x_N - I}{\beta}} dx_N \\ &= \frac{1}{\beta^2} \int_I^\infty (x_N - I) e^{tx_N} e^{-\frac{x-I}{\beta}} dx_N \\ &= \frac{1}{\beta^2} \int_I^\infty (x_N - I) e^{-\frac{x_N - I}{\beta} + tx_N} dx_N \\ &= \frac{1}{\beta^2} \int_I^\infty (x - I) e^{-\frac{x_N - I}{\beta} + tI + t(x_N - I)} dx_N \\ &= \frac{e^{tI}}{\beta^2} \int_I^\infty (x_N - I) e^{(t-\frac{1}{\beta})(x_N - I)} dx_N. \end{aligned}$$

Let $u = x_N - I$, such that $du = dx_N$. We then have,

$$\begin{aligned} M_{X_N}(t) &= \frac{e^{tI}}{\beta^2} \int_0^\infty u e^{(t-\frac{1}{\beta})u} du \\ &= \frac{e^{tI}}{\beta^2} \cdot \frac{1}{(\frac{1}{\beta} - t)^2}, \int_0^\infty u e^{-\lambda u} du = \frac{1}{\lambda^2}, \ \text{ for } \lambda > 0, \lambda = \frac{1}{\beta} - t \\ &= \frac{e^{tI}}{(1-\beta t)^2}, \quad \text{for } t < \frac{1}{\beta}. \end{aligned}$$

3.4. Survival function and hazard rate function

The SF $S(x_N;\beta)$ is commonly employed in reliability analysis to represent the probability that a system continues to function beyond a specified time x. The SF for the NMED is given by

$$S(x_N;\beta) = 1 - F(x_N;\beta) = \left(1 + \frac{x_N - I}{\beta}\right) e^{-\frac{x_N - I}{\beta}}. \tag{3.4}$$

The HRF, also known as the failure rate or instantaneous failure rate, quantifies the likelihood that a system or component will fail at a particular time x, given that it has been functioning without failure up to that time. Mathematically, the HRF is defined as the ratio of the PDF to the SF. The HRF for the NMED is given by

$$HRF(x_N;\beta) = \frac{f(x_N;\beta)}{S(x_N;\beta)} = \frac{x_N - I}{\beta(\beta + x_N - I)}. \tag{3.5}$$

Figure 3 shows the SF and HRF plots for some distribution parameter values for the cases $(\beta = 2, I = 1.55), (\beta = 3, I = 1.55), (\beta = 2, I = 2.59), (\beta = 3, I = 2.59), (\beta = 2, I = 3.54), (\beta = 3, I = 3.54), (\beta = 2, I = 4.91),$ and $(\beta = 3, I = 4.91)$.

From the graph, it is evident that the SF curves decreases at varying rates, which depend on the values of the scale parameter β and the indeterminacy I. For example, $\beta = 3$ results in a slower decline, indicating a longer operational lifespan and greater reliability. In contrast, a lower value such as $\beta = 2$, leads to a faster decline, suggesting a shorter lifespan and quicker system failure. Initially, both systems have a high survival probability but, over time, the survival probability decreases more rapidly for smaller values of β. Therefore, the system with $\beta = 3$ is more durable and reliable than the one with $\beta = 2$.

For the HRF plots, the curves tend to rise over time, indicating that the likelihood of failure grows as the system ages. However, the rate of this increase varies, depending on the scale parameter β. A system with a larger β (i.e., more robust) shows a slower increase in the HRF, implying that it is less likely to fail quickly. On the other hand, a system with a smaller β experiences a steeper increase in the HRF, suggesting that it is more prone to failure as time progresses.

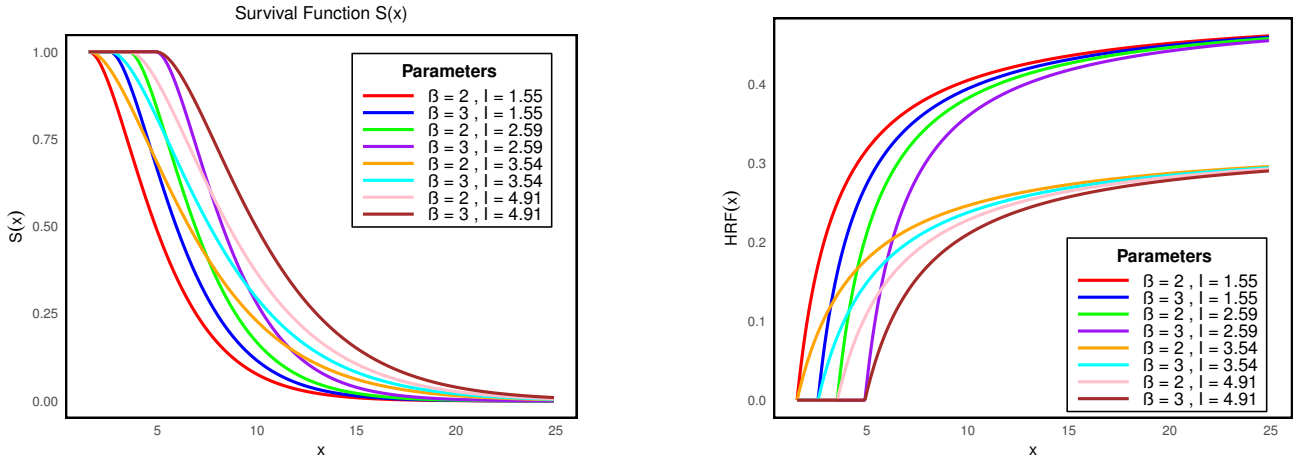

Figure 3. SF and HRF plots of the NMED for some parameter values.

3.5. Quantile function

The quantile function is the inverse of the CDF. For the NMED, it is given by

$$Q(p) = I + \beta\left(-W\left(-(p-1)e^{-1}\right) - 1\right),$$

where $W(\cdot)$ is the Lambert function, $W(x)e^{W(x)} = x$, and $Q(p) = F_{x_N}^{-1}(p)$.

3.6. Cumulative hazard function and mean residual life function

The CHF represents the total accumulated risk of failure up to a specified time x. It is the integral of the HRF over time. For the NMED, the CHF is given by

$$\begin{aligned} CHF(x_N;\beta) &= -\ln S(x_N;\beta) \\ &= -\ln\left(1 + \frac{x_N - I}{\beta}\right) + \frac{x_N - I}{\beta}. \end{aligned} \tag{3.6}$$

The MRLF of the NMED provides the expected remaining lifetime of a system or component, given that it has survived up to a specific time x. The MRLF for the NMED is defined as follows.

Theorem 3. The MRLF of the NMED is defined as

$$r_N(t) = \beta + (t - I). \tag{3.7}$$

Proof. Using the MRLF's definition

$$r_N(t) = E[X_N - t \mid X_N > t] = \frac{\int_t^\infty S(x_N)\,dx}{S(t)},$$

with the SF, we have

$$\begin{aligned} r_N(t) &= \frac{\int_t^\infty e^{-\frac{x_N - I}{\beta}} \left(1 + \frac{x_N - I}{\beta}\right) dx_N}{e^{-\frac{t-I}{\beta}} \left(\frac{\beta + t - I}{\beta}\right)} \\ &= \frac{\beta e^{-\frac{t-I}{\beta}} \left(\frac{\beta + t - I}{\beta}\right) + \beta e^{-\frac{t-I}{\beta}}}{e^{-\frac{t-I}{\beta}} \left(\frac{\beta + t - I}{\beta}\right)} \\ &= \beta + (t - I). \end{aligned}$$

This means that the MRLF is linear in t, increasing at a constant rate as t increases.

Figure 4 presents the plots of the CHF and MRLF for the NMED for different values of β and I.

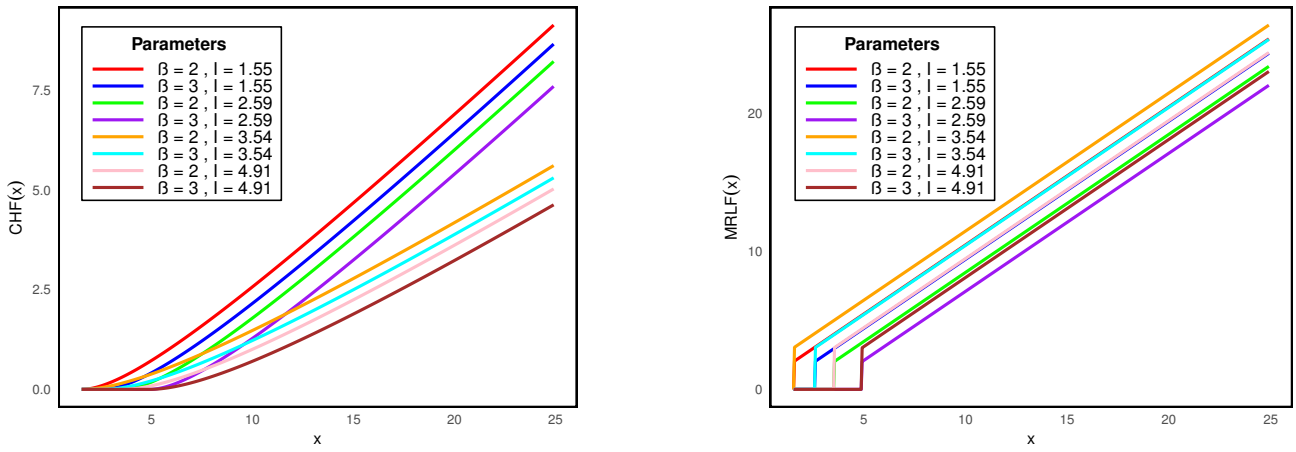

Figure 4. CHF and MRLF plots of the NMED for some parameter values.

3.7. Mills ratio and elasticity

The Mills ratio is the ratio of the complementary CDF to the PDF, which can be expressed as

$$M(x_N) = \frac{1 - F(x_N;\beta)}{f(x_N;\beta)} = \beta + \frac{\beta^2}{x_N - I}.$$

The elasticity, in the context of probability distributions, measures the responsiveness of the PDF to changes in the variable x_N. Specifically, it quantifies the relative change in the PDF as a result of a relative change in x_N. For a given PDF $f(x_N;\beta)$, the elasticity with respect to x_N is defined as

$$E_{x_N} = \frac{d \ln f(x_N;\beta)}{d \ln x_N} = \frac{1}{x_N - I} - \frac{1}{\beta}.$$

Figure 5 displays the plots of the Mills ratio and elasticity for the NMED across various values of β and I. It is evident that both functions exhibit a decreasing trend for all the parameter values examined.

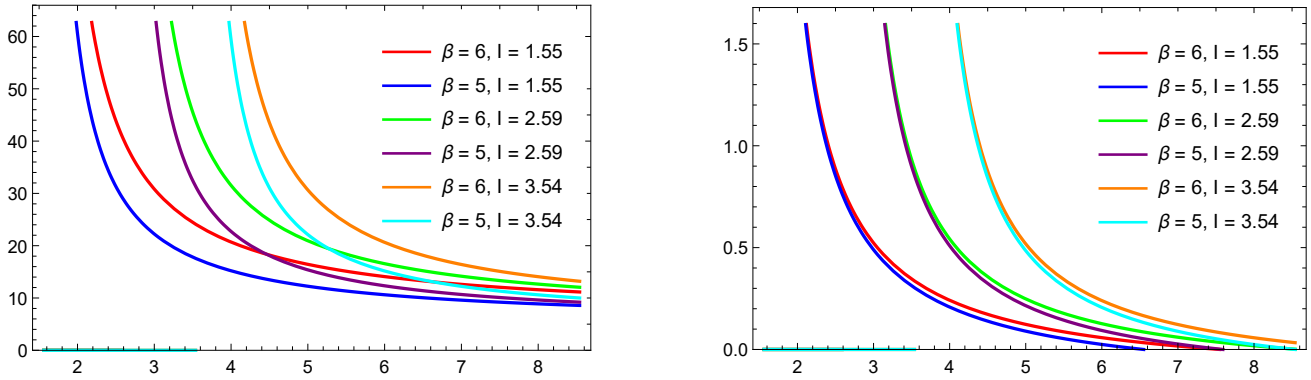

Figure 5. Mills ratio and elasticity plots of the NMED for selected parameter values.

4. Extropy and entropy

4.1. Extropy

Lad et al. [27] defined the extropy of a random variable X, with $f(x)$, as:

$$J(X) = -\frac{1}{2}\int_{-\infty}^{\infty} f^2(x)\,dx.$$

Balakrishnan et al. [28] and Gupta et al. [29] offered the following concept of weighted extropy:

$$J_w(X) = -\frac{1}{2}\int_{-\infty}^{\infty} x f^2(x)\,dx.$$

The cumulative residual extropy is defined by

$$J_c(X) = -\frac{1}{2}\int_{-\infty}^{\infty} (1 - F(x))^2\,dx.$$

Theorem 4. Let X_N be a random variable follows the NMED, in which case the extropy, weighted extropy, and cumulative residual extropy are, respectively, given by

$$J(X_N) = -\frac{1}{8\beta},\ \beta > 0,$$
$$J_w(X_N) = -\frac{3\beta + 2I}{16\beta},\ \beta > 0,$$
$$J_c(X_N) = -\frac{5\beta}{8}.$$

Proof. We will prove $J(X_N)$, and the proofs of $J_w(X_N)$ and $J_c(X_N)$ are similar. Given the PDF defined in Eq (2.1), we have

$$\begin{aligned} J(X_N) &= -\frac{1}{2}\int_I^\infty f^2(x_N;\beta)\,dx_N \\ &= -\frac{1}{2}\int_I^\infty \frac{(x_N-I)^2}{\beta^4} e^{-2\frac{x_N-I}{\beta}}\,dx_N. \end{aligned}$$

If we let $u = x_N - I$, then as $x_N = I$, $u = 0$, $x_N \to \infty$, $u \to \infty$, $dx_N = du$, and $x_N - I = u$, the integral becomes

$$\begin{aligned} J(X_N) &= -\frac{1}{2}\int_0^\infty \frac{u^2}{\beta^4} e^{-2\frac{u}{\beta}}\,du = -\frac{1}{2\beta^4}\int_0^\infty u^2 e^{-2\frac{u}{\beta}}\,du \\ &= -\frac{1}{2\beta^4}\beta^3\int_0^\infty t^2 e^{-2t}\,dt, t = \frac{u}{\beta}, u = \beta t, du = \beta\,dt, \frac{u}{\beta} = t, e^{-2\frac{u}{\beta}} = e^{-2t} \\ &= -\frac{1}{2\beta^4}\beta^3\frac{1}{4}, u = 0 \to t = 0, u \to \infty \to t \to \infty, \int_0^\infty t^n e^{-at}\,dt = \frac{\Gamma(n+1)}{a^{n+1}} \\ &= -\frac{1}{8\beta}. \end{aligned}$$

Remark. It is of interest to note here that the $J(X_N)$ and $J_c(X_N)$ of the NMED are free of I, and they are similar to their counterparts of the base MED, but $J_w(X_N)$ depends on I.

4.2. Shannon entropy

Theorem 5. The Shannon entropy $H_s(X_N)$ of a continuous random variable X_N with $f(x_N;\beta)$ is given by

$$H_s(X_N) = 1 + \gamma + \ln(\beta) + \frac{2i\pi e^{w/\beta}\left(w^2 - \beta^2 + \beta w\right)}{\beta^2},\ \beta > 0, \tag{4.1}$$

where γ is the Euler–Mascheroni constant.

Proof. The Shannon entropy is defined as

$$\begin{aligned}
H_s(X_N) &= -\int_I^\infty f(x_N;\beta)\ln f(x_N;\beta)\,dx_N \\
&= -\int_I^\infty \frac{(x_N-I)}{\beta^2}e^{-\frac{x_N-I}{\beta}}\left(\ln(x_N-I)-2\ln\beta-\frac{x_N-I}{\beta}\right)dx_N \\
&= -\int_I^\infty \frac{(x_N-I)}{\beta^2}e^{-\frac{x_N-I}{\beta}}\ln(x_N-I)dx_N+2\ln\beta\int_I^\infty \frac{(x_N-I)}{\beta^2}e^{-\frac{x_N-I}{\beta}}dx_N \\
&+\int_I^\infty \frac{(x_N-I)^2}{\beta^3}e^{-\frac{x_N-I}{\beta}}dx \\
&= -\int_I^\infty \frac{(x_N-I)}{\beta^2}e^{-\frac{x_N-I}{\beta}}\ln(x_N-I)dx_N+2\ln\beta\int_I^\infty \frac{(x_N-I)}{\beta^2}e^{-\frac{x_N-I}{\beta}}dx_N \\
&+\int_I^\infty \frac{(x_N-I)^2}{\beta^3}e^{-\frac{x_N-I}{\beta}}dx \\
&= -\log(\beta)+\frac{2i\pi e^{w/\beta}\left(-\beta^2+w^2+\beta w\right)}{\beta^2}+\gamma-1+2ln(\beta)+2 \\
&= 1+\gamma+\ln(\beta)+\frac{2i\pi e^{w/\beta}\left(w^2-\beta^2+\beta w\right)}{\beta^2}.
\end{aligned}$$

The proof is done using the integrals

$$\int_0^\infty ue^{-u/\beta}\ln u\,du=\beta^2(\ln\beta-\gamma+1),\ \int_0^\infty ue^{-u/\beta}\,du=\beta^2,\ \ \int_0^\infty u^2e^{-u/\beta}\,du=2\beta^3.$$

4.3. Rényi entropy

Theorem 6. The Rényi entropy of order α for a continuous random variable X_N with the PDF $f(x_N)$ is defined as

$$H_\alpha(X_N)=\frac{1}{1-\alpha}\left(\ln\Gamma(\alpha+1)+(1-\alpha)\ln\beta-(\alpha+1)\ln\alpha\right). \tag{4.2}$$

Proof. It is well known that

$$\begin{aligned}
H_\alpha(X_N) &= \frac{1}{1-\alpha}\ln\int_I^\infty f(x_N;\beta)^\alpha dx_N,\quad \alpha>0,\alpha\neq 1 \\
&= \frac{1}{1-\alpha}\ln\int_I^\infty \frac{(x_N-I)^\alpha}{\beta^{2\alpha}}e^{-\alpha\frac{x_N-I}{\beta}}dx_N \\
&= \frac{1}{1-\alpha}\ln\frac{\Gamma(\alpha+1)}{\beta^{2\alpha}\left(\frac{\alpha}{\beta}\right)^{\alpha+1}},\int_0^\infty u^me^{-\lambda u}du=\frac{\Gamma(m+1)}{\lambda^{m+1}},\quad \text{for } \lambda>0 \\
&= \frac{1}{1-\alpha}\ln\left(\frac{\Gamma(\alpha+1)\beta^{1-\alpha}}{\alpha^{\alpha+1}}\right),u=x_N-I,m=\alpha,\text{and }\lambda=\frac{\alpha}{\beta} \\
&= \frac{1}{1-\alpha}\left(\ln\Gamma(\alpha+1)+(1-\alpha)\ln\beta-(\alpha+1)\ln\alpha\right).
\end{aligned}$$

5. Parameter estimation

5.1. Order statistics

Consider a random sample of size m, denoted as $X_{N1}, X_{N2}, ..., X_{Nm}$, drawn from the PDF defined in Eq (2.1) and the CDF given in Eq (2.2). The PDF of the j^{th}-order statistic, $X_{N(j:m)}$, is then expressed as

$$\begin{aligned} f_{(j:m)}(x_N;\beta) &= \frac{n!}{(j-1)!(n-j)!}[F(x_N;\beta)]^{j-1}[1-F(x_N;\beta)]^{n-j}f(x_N;\beta) \\ &= \frac{m!(x_N-I)\left(\frac{e^{\frac{I-x_N}{\beta}}(I-\beta-x_N)}{\beta}+1\right)^{j-1}\left(\frac{e^{\frac{I-x_N}{\beta}}(\beta+x_N-I)}{\beta}\right)^{m-j+1}}{\beta\Gamma(j)\Gamma(m-j+1)(\beta+x_N-I)}, x_N > I,\ \beta > 0. \end{aligned} \tag{5.1}$$

The PDFs for the minimum and maximum order statistics are, respectively, expressed as

$$f_{(1:m)}(x_N;\beta) = \frac{m!}{\beta\Gamma(m)(\beta+x_N-I)}(x_N-I)\left(\frac{e^{\frac{I-x_N}{\beta}}(\beta+x_N-I)}{\beta}\right)^m, \tag{5.2}$$

$$f_{(m:m)}(x_N;\beta) = \frac{m!}{\beta^2\Gamma(m)}(x_N-I)e^{\frac{I-x_N}{\beta}}\left(\frac{e^{\frac{I-x_N}{\beta}}(-\beta-x_N+I)}{\beta}+1\right)^{m-1}. \tag{5.3}$$

The r^{th} moments of the minimum and maximum order statistics are, respectively, given by

$$E_{(1:m)}(X_N^r) = \frac{m!\beta^{r+1}}{\Gamma(m)}\sum_{k=0}^{r}\binom{r}{k}I^{r-k}\int_0^\infty t^{k+1}(1+t)^{m-1}e^{-mt}dt$$

$$E_{(m:m)}(X_N^r) = \sum_{k=0}^{r}\binom{r}{k}I^{r-k}\cdot\frac{m!}{\beta^2\Gamma(m)}\int_0^\infty u^{k+1}e^{-u/\beta}\left(1-\frac{\beta+u}{\beta}e^{-u/\beta}\right)^{m-1}du, u = x_N - I.$$

5.2. Maximum likelihood estimation

ML estimation is a widely used statistical method for estimating unknown model parameters by determining the values that maximize the likelihood of the observed data. In this study, we employ the ML estimation approach to estimate the unknown parameter β in the PDF of the NMED. Given n observations $x_{N1}, x_{N2}, \ldots, x_{Nn}$, the likelihood function is formulated as

$$L(\beta) = \prod_{i=1}^{n} f(x_{Ni};\beta) = \prod_{i=1}^{n}\frac{x_{Ni}-I}{\beta^2}e^{-\frac{x_{Ni}-I}{\beta}}.$$

The log-likelihood function is given by

$$\log L(\beta) = \sum_{i=1}^{n}\left\{\log(x_{Ni}-I) - \log(\beta^2)\right\} - \sum_{i=1}^{n}\frac{x_{Ni}-I}{\beta}$$

$$= \sum_{i=1}^{n}\log\frac{x_{Ni}-I}{\beta^2} - \sum_{i=1}^{n}\frac{x_{Ni}-I}{\beta}.$$

By setting the partial derivative of $\log L(\beta)$ as

$$\frac{\partial}{\partial\beta}\log L(\beta) = \sum_{i=1}^{n} -\frac{2}{\beta} + \sum_{i=1}^{n} \frac{x_{Ni} - I}{\beta^2} = 0.$$

The maximum likelihood estimate (MLE) of β is

$$\hat{\beta} = \frac{\bar{X_N} - I}{2}. \tag{5.4}$$

6. Simulation studies

A simulation study is a statistical approach used to assess the performance, accuracy, or reliability of statistical methods, models, or algorithms by generating and analyzing artificial data. Rather than depending on real-world data, it utilizes synthetic datasets based on specific assumptions or probability distributions. This allows researchers to examine how a method performs in controlled, repeatable scenarios. Simulation studies are an essential tool in contemporary statistics and data science, offering a versatile and effective framework for exploring the behavior of statistical techniques across different conditions. We perform a simulation study to evaluate the effectiveness of the proposed estimators for the NMED. A total of 1000 samples of different sizes (n = 50, 100, 150, 200, and 300) are generated from the NMED using a random number generator. To assess the properties of the proposed estimator, we utilize the absolute mean bias (ABias), mean squared error (MSE), and mean relative error (MRE) as evaluation metrics. These measures are defined, respectively, as follows:

$$ABias(\hat{\beta}) = \left|\frac{1}{n}\sum_{i=1}^{n}(\hat{\beta}_i - \beta_i)\right|, MSE(\hat{\beta}) = \frac{1}{n}\sum_{i=1}^{n}(\hat{\beta}_i - \beta_i)^2, MRE(\hat{\beta}) = \frac{1}{n}\sum_{i=1}^{n}\frac{|\hat{\beta}_i - \beta_i|}{|\beta_i|},$$

where $\hat{\beta}_i$ is the estimated value of β, β_i is the true value of β, and n is the number of observations. The results of simulation study are listed in Table 1.

Table 1. MLE, bias, MSE, and MRE of parameter estimates of NMED for various values of β and I.

n	**MLE**	**Bias**	**MSE**	**MRE**	**MLE**	**Bias**	**MSE**	**MRE**
	$\beta = 1.20,\ I = 0.02$				$\beta = 2.50,\ I = 0.02$			
50	1.201740	0.001740	0.013810	0.078239	2.503630	0.003630	0.059935	0.078234
100	1.200984	0.000984	0.007129	0.056161	2.502058	0.002058	0.030941	0.056155
150	1.201168	0.001168	0.004951	0.047101	2.502442	0.002442	0.021485	0.047093
200	1.199714	0.000286	0.003543	0.039292	2.499412	0.000588	0.015374	0.039284
300	1.199831	0.000169	0.002458	0.033048	2.499655	0.000345	0.010665	0.033039
400	1.201026	0.001026	0.001796	0.028120	2.502145	0.002145	0.007791	0.028110
500	1.200200	0.000200	0.001423	0.025224	2.500422	0.000422	0.006175	0.025214
	$\beta = 0.50,\ I = 0.02$				$\beta = 7.50,\ I = 4.70$			
50	0.500725	0.000725	0.002397	0.078234	7.510882	0.010881	0.539425	0.078235
100	0.500410	0.000410	0.001238	0.056153	7.506163	0.006163	0.278475	0.056156
150	0.500486	0.000486	0.000859	0.047093	7.507312	0.007312	0.193369	0.047094
200	0.499880	0.000120	0.000615	0.039283	7.498221	0.001779	0.138369	0.039284
300	0.499928	0.000072	0.000427	0.033039	7.498949	0.001051	0.095995	0.033040
400	0.500426	0.000426	0.000312	0.028112	7.506420	0.006420	0.070128	0.028112
500	0.500081	0.000081	0.000247	0.025215	7.501251	0.001251	0.055578	0.025215

From Table 1, the following points can be concluded.

- As the sample size increases, the MLE for β becomes more precise and approaches the true value. For example, at $\beta = 1.20$, the MLE at $n = 50$ is 1.201740, while at $n = 500$, it is 1.200200.
- The bias decreases with an increasing sample size. At $n = 50$, the bias for $\beta = 1.20$ is 0.001740, but at $n = 500$, it drops to 0.000200, becoming almost negligible. Moreover, the MSE decreases as the sample size increases. For instance, at $n = 50$, the MSE for $\beta = 1.20$ is 0.013810, but by $n = 500$, it decreases to 0.001423. Similarly, for $\beta = 0.50$, the MSE reduces from 0.002397 at $n = 50$ to 0.000247 at $n = 500$.
- The MRE shows a clear reduction with increasing sample size. For $\beta = 1.20$, the MRE starts at 0.078239 for $n = 50$ and drops to 0.025224 at $n = 500$, indicating improved relative accuracy with larger sample sizes. At $\beta = 7.5$, the MRE for $n = 50$ is 0.078235, but by $n = 500$, it reduces to 0.025215.
- For the comparison of different smaller, values of β (e.g., $\beta = 0.50$) tend to yield a smaller bias, MSE, and MRE compared with larger values of β. For instance, at $n = 50$, the bias for $\beta = 0.50$ is 0.000725, while for $\beta = 7.5$, the bias is 0.010881, showing that larger values of β lead to higher estimation errors. Similarly, the MSE at $\beta = 0.50$ is 0.002397, but for $\beta = 7.5$, it jumps to 0.539425 at $n = 50$, indicating a larger error at higher values of β.
- The trend of decreasing bias, MSE, and MRE with increasing n is consistent across all β values. For example, at $\beta = 2.5$, the MSE decreases from 0.059935 at $n = 50$ to 0.006175 at $n = 500$, and similarly, at $\beta = 7.5$, the MSE decreases from 0.539425 at $n = 50$ to 0.055578 at $n = 500$, showing that larger sample sizes lead to more accurate estimates, regardless of the value of β.
- For large values of β, the estimation errors are significantly higher. For example, at $\beta = 7.5$, the

bias at $n = 50$ is 0.010881, the MSE is 0.539425, and the MRE is 0.078235. In contrast, for $\beta = 0.50$, the bias at $n = 50$ is only 0.000725, the MSE is 0.002397, and the MRE is 0.078234, illustrating that smaller values of β result in more accurate estimates.

- As expected, larger sample sizes reduce the impact of random variation on parameter estimation. At $n = 500$, the MLE for $\beta = 2.5$ is 2.500422, with a very small bias of 0.000422 and a low MSE of 0.006175, which highlights the accuracy achieved with large values of n. In contrast, for smaller sample sizes such as $n = 50$, the MSE for $\beta = 2.5$ is higher at 0.059935.

7. Application

This section focuses on estimating the parameters of the proposed distribution using a real-world dataset. To assess the goodness-of-fit, we consider the log-likelihood value (L), the Akaike information criterion (AIC) introduced by [30], and the Bayesian information criterion (BIC) proposed by [31]. These criteria are defined as follows:

$$AIC = 2k - 2\ln(L), \quad BIC = k\ln(n) - 2\ln(L),$$

where k represents the number of estimated parameters in the model, and n is the total number of observations.

A model is considered to provide a better fit when the log-likelihood value is maximized while the AIC and BIC values are minimized. For illustration purposes, a real-life dataset is analyzed and investigated on the basis of suggested NMED in a comparison with alternative models. To ensure a fair and meaningful comparison, the neutrosophic representation was unified in this study by applying a common transformation framework to all competing models. The neutrosophic Lindley distribution (NLiD) of [32] and neutrosophic inverse gamma distribution (NIGD) of [33] were re-parameterized using the same indeterminacy parameter I as adopted in the formulation of the proposed NMED, whereas the neutrosophic exponential distribution (NED) of [26] and neutrosophic gamma distribution (NGD) of [26] follow an equivalent neutrosophic structure consistent with this framework. This unification allows a direct comparison of the fitted neutrosophic models. Since the NMED is a one-parameter distribution, it was compared accordingly with the corresponding one-parameter NGD and NIGD.

7.1. Example 1

The dataset analyzed in this study corresponds to child mortality rates and is obtained from [34]. It consists of interval estimates of infant death rates for children under the age of five years. The dataset is [31.53, 31.81], [29.33, 30.08], [27.23, 28.67], [25.09, 26.34], [24.20, 24.88], [22.00, 23.50], [20.66, 22.09], [19.74, 20.59], [18.57, 20.03], [18.04, 18.77], [16.89, 17.89], [15.92, 16.21], [14.51, 15.92], [13.92, 14.71], [12.73, 14.32], [12.20, 13.35], [11.18, 12.68], [10.21, 11.75], [10.12, 11.03], [9.12, 10.69], [8.47, 9.42], [8.59, 9.28], [7.65, 9.03], [7.77, 8.59], [7.23, 7.98], and [6.81, 8.06]. The parameters of the NMED are estimated using the MLE method, and its goodness of fit is assessed to evaluate the model's performance.

Figure 6 presents graphical tools for comparing the dataset with a theoretical distribution, including the probability–probability (P-P) plot, quantile–quantile (Q-Q) plot, and box and density plots for the child mortality rate dataset.

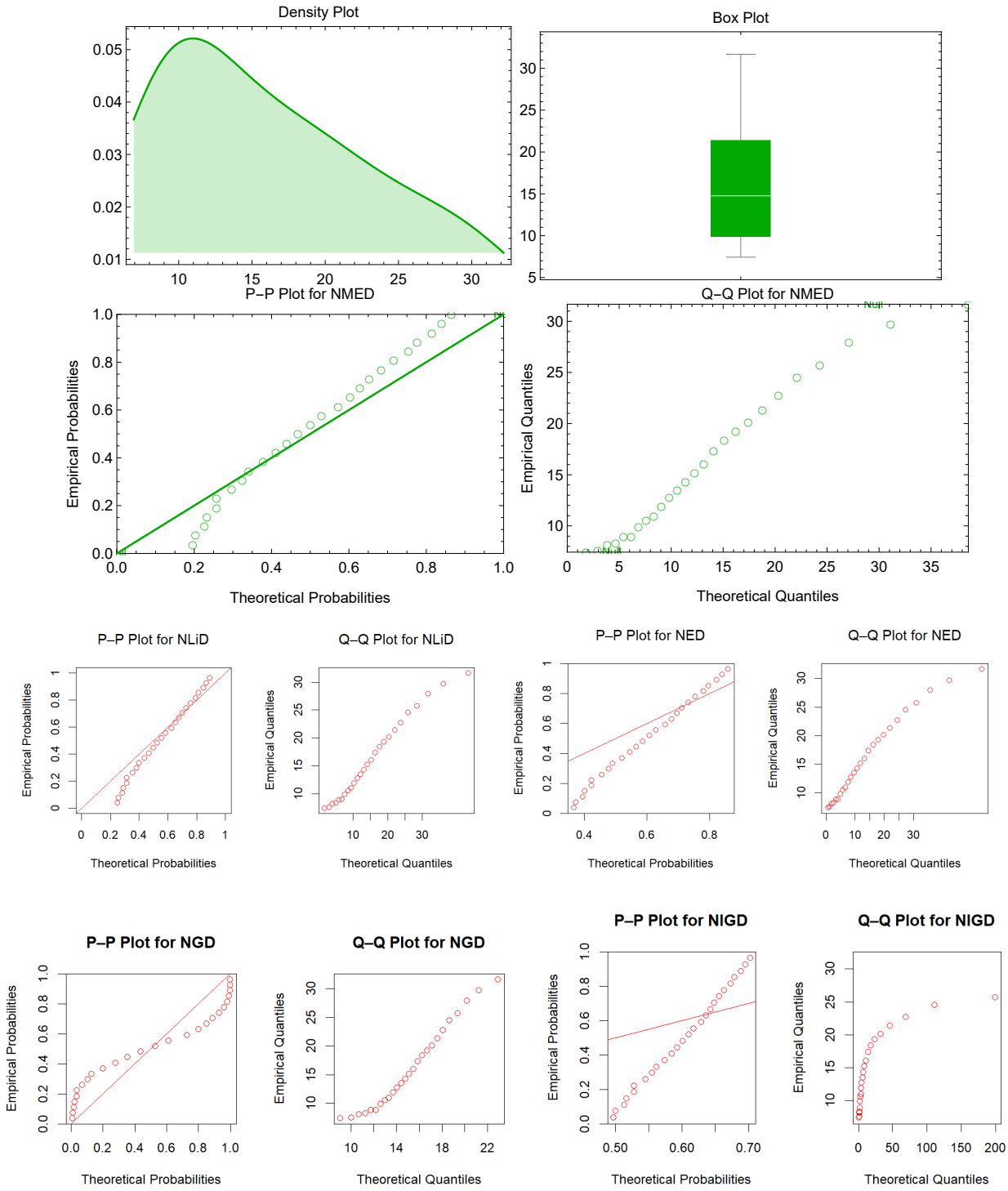

Figure 6. The density, box, P-P, and Q-Q plots for the child mortality rate dataset.

The goodness of fit findings are summarized in Table 2, which presents the ML estimates and the model's adequacy criteria (AIC and BIC) for the child mortality rate dataset.

Table 2. MLEs, L, AIC, and BIC measures for the child mortality rate dataset with $I = 0.01$.

Model	MLE	L	AIC	BIC
NMED	$\hat{\beta}$ = [7.874, 8.4117]	[−90.388, −91.709]	[182.78, 185.42]	[184.03, 186.68]
NLiD	$\hat{\vartheta}$ = [0.12019, 0.11286]	[−91.469, −92.781]	[184.94, 187.56]	[186.20, 188.82]
NED	$\hat{\lambda}$ = [0.063505, 0.059446]	[−97.675, −99.392]	[197.35, 200.78]	[198.61, 202.04]
NGD	$\hat{\theta}$ = [14.661, 15.861]	[−99.473, −97.306]	[200.95, 196.61]	[202.20, 197.87]
NIGD	$\hat{\alpha}$ = [0.38805, 0.37772]	[−119.22, −121.96]	[240.44, 245.92]	[241.70, 247.17]

It is revealed that the AIC and BIC values for the NMED are lower compared with other existing distributions indicating a better fit for the child mortality rate dataset.

From the results presented in Table 2, it can be seen that the proposed NMED is more accurate as compared with other existing distributions in fitting the child mortality rate dataset.

8. Conclusions

In conclusion, this paper successfully extends traditional statistical distribution theory by incorporating the effects of uncertainty, ambiguity, and imprecision through the development of the NMED. The NMED offers a more robust framework for handling real-world problems involving indeterminacy. The study provides comprehensive mathematical formulations for key properties of the NMED, including its quantile function, Mills ratio, elasticity, moments, and various information measures such as Shannon and Rényi entropies. Additionally, the NMED's SF, HRF, CHF, and MRLF are thoroughly explored, and visualizations provide further insights. By employing ML estimation and conducting a simulation study, the effectiveness and reliability of the NMED in real-world scenarios are established. The comparison with the other neutrosophic distributions demonstrates the superior performance of the NMED in modeling the child mortality rate dataset. This study highlights the practical advantages of the NMED in situations involving uncertainty and its potential for broader applications in statistical modeling. Future works may focus on studying the complexity of the NMED through Bayesian methods. In this context, Bayesian inference can be applied for parameter estimation, and the model's adequacy may be evaluated using the deviance information criterion.

Author contributions

R. Maya, M. R. Irshad and A. S. Aparna: Conceptualization, Methodology, Software, Formal analysis, Writing–original draft, Writing–review & editing and Visualization. Amer I. Al-Omari and Ghadah Alomani: Conceptualization, Validation, Formal analysis, Writing–original draft, Writing–review & editing, Visualization. Ghadah Alomani: Funding. All authors have read and approved the final version of the manuscript for publication.

Use of Generative-AI tools declaration

The authors declare they have not used Artificial Intelligence (AI) tools in the creation of this article.

Acknowledgments

Princess Nourah bint Abdulrahman University Researchers Supporting Project number (PNURSP2025R226), Princess Nourah bint Abdulrahman University, Riyadh, Saudi Arabia.

Data availability

The dataset used in this paper are available within the manuscript.

Conflict of interest

The authors affirm that there are no conflicts of interest.

References

1. R. A. Aldallal, E. Hussam, The new extended-X exponentiated inverted Weibull distribution: statistical inference and application to carbon data, *Appl. Math. Inform. Sci.*, **18** (2024), 737–747. http://doi.org/10.18576/amis/180406
2. A. I. Al-Omari, A. R. A. Alanzi, S. S. Alshqaq, The unit two parameters Mirra distribution: reliability analysis, properties, estimation and applications, *Alex. Eng. J.*, **92** (2024), 238–253. https://doi.org/10.1016/j.aej.2024.02.063
3. A. I. Al-Omari, R. Alsultan, G. Alomani, Asymmetric right-skewed size-biased Bilal distribution with mathematical properties, reliability analysis, inference and applications, *Symmetry*, **15** (2023), 1578. https://doi.org/10.3390/sym15081578
4. M. R. Irshad, M. Ahammed, R. Maya, A. I. Al-Omari, Marshall-Olkin Bilal distribution with associated minification process and acceptance sampling plans, *Hacet. J. Math. Stat.*, **53** (2024), 201–229. https://doi.org/10.15672/hujms.1143156
5. M. R. Irshad, S. Aswathy, R. Maya, A. I. Al-Omari, G. Alomani, A flexible model for bounded data with bathtub shaped hazard rate function and applications, *AIMS Math.*, **9** (2024), 24810–24831. https://doi.org/10.3934/math.20241208
6. F. Smarandache, Neutrosophic set-a generalization of the intuitionistic fuzzy set, *International Journal of Pure and Applied Mathematics*, **24** (2005), 287.
7. M. B. Zeina, A. Hatip, Neutrosophic random variables, *Neutrosophic Sets and Systems*, **39** (2021), 44–52.
8. S. K. Patro, F. Smarandache, The neutrosophic statistical distribution, more problems, more solutions, *Neutrosophic Sets and Systems,* **12** (2016), 73–79.
9. R. Alhabib, M. M. Ranna, H. Farah, A. A. Salama, Some neutrosophic probability distributions, *Neutrosophic Sets and Systems*, **22** (2018), 30–38.

10. K. F. H. Alhasan, F. Smarandache, Neutrosophic Weibull distribution and neutrosophic family Weibull distribution, *Neutrosophic Sets and Systems*, **28** (2019), 15.

11. A. R. Alanzi, M. R. Irshad, M. Johny, A. I. Al-Omari, H. Alrweili, Neutrosophic Poisson moment exponential distribution: properties and applications, *Maejo Int. J. Sci. Tech.*, **19** (2025), 133–149.

12. R. A. K. Sherwani, M. Naeem, M. Aslam, M. Raza, M. Abid, S. Abbas, Neutrosophic beta distribution with properties and applications, *Neutrosophic Sets and Systems*, **41** (2021), 209–214.

13. Z. Khan, A. Al-Bossly, M. M. Almazah, F. S. Alduais, On statistical development of neutrosophic gamma distribution with applications to complex data analysis, *Complexity*, **2021** (2021), 3701236. https://doi.org/10.1155/2021/3701236

14. Z. Khan, M. Gulistan, N. Kausar, C. Park, Neutrosophic Rayleigh model with some basic characteristics and engineering applications, *IEEE Access*, **9** (2021), 71277–71283. https://doi.org/10.1109/ACCESS.2021.3078150

15. B. M. Nayana, K. K. Anakha, V. M. Chacko, M. Aslam, M. Albassam, A new neutrosophic model using Dus-Weibull transformation with application, *Complex Intell. Syst.*, **8** (2022), 4079–4088. https://doi.org/10.1007/s40747-022-00698-6

16. M. B. Zeina, M. Abobala, A. Hatip, S. Broumi, S. J. Mosa, Algebraic approach to literal neutrosophic Kumaraswamy probability distribution, *Neutrosophic Sets and Systems*, **54** (2023), 124–138.

17. R. Alsultan, A. I. Al-Omari, Neutrosophic Quasi-XLindley distribution with applications of COVID-19 data, *Neutrosophic Sets and Systems*, **82** (2025), 530–541.

18. L. A. Al-Essa, F. Jamal, S. Shafiq, S. Khan, Q. Abbas, R. A. K. Sherwani, et al., Properties and applications of neutrosophic Burr XII distribution, *Int. J. Comput. Intell. Syst.*, **18** (2025), 10. https://doi.org/10.1007/s44196-024-00721-3

19. R. Alhabib, A. A. Salama, Using moving averages to pave the neutrosophic time series, *International Journal of Neutrosophic Science*, **3** (2020), 14–20. https://doi.org/10.5281/zenodo.3732611

20. M. Aslam, A new sampling plan using neutrosophic process loss consideration, *Symmetry*, **10** (2018), 132. https://doi.org/10.3390/sym10050132

21. S. T. Dara, M. Aḥmad, *Recent advances in moment distribution and their hazard rates*, Lap Lambert Academic Publishing, 2012.

22. S. A. Hasnain, Z. Iqbal, M. Ahmad, On exponentiated moment exponential distribution, *Pak. J. Statist.*, **31** (2015), 267–280.

23. M. A. Ul Haq, R. M. Usman, S. Hashmi, A. I. Al-Omeri, The Marshall-Olkin length-biased exponential distribution and its applications, *J. King Saud Univ. Sci.*, **31** (2019), 246–251. https://doi.org/10.1016/j.jksus.2017.09.006

24. S. Hashmi, M. A. Ul Haq, R. M. Usman, A generalized exponential distribution with increasing, decreasing and constant shape hazard curves, *Electron. J. Appl. Stat. Anal.*, **12** (2019), 223–244. https://doi.org/10.1285/i20705948v12n1p223

25. R. Maya, J. Huang, M. R. Irshad, F. Zhu, On Poisson moment exponential distribution with associated regression and INAR(1) process, *Ann. Data Sci.*, **11** (2024), 1741–1759. https://doi.org/10.1007/s40745-023-00476-2

26. C. Granados, A. K. Das, B. Das, Some continuous neutrosophic distributions with neutrosophic parameters based on neutrosophic random variables, *Advances in the Theory of Nonlinear Analysis and its Application*, **6** (2022), 380–389. https://doi.org/10.31197/atnaa.1056480

27. F. Lad, G. Sanfilippo, G. Agro, Extropy: complementary dual of entropy, *Statist. Sci.*, **30** (2015), 40–58. https://doi.org/10.1214/14-STS430

28. N. Balakrishnan, F. Buono, M. Longobardi, On weighted extropies, *Commun. Stat.-Theor. Meth.*, **51** (2022), 6250–6267. https://doi.org/10.1080/03610926.2020.1860222

29. N. Gupta, S. K. Chaudhary, On general weighted extropy of ranked set sampling, *Commun. Stat.-Theor. Meth.*, **53** (2024), 4428–4441. https://doi.org/10.1080/03610926.2023.2179888

30. H. Akaike, A new look at the statistical model identification, *IEEE Trans. Automat. Contr.*, **19** (2003), 716–723. https://doi.org/10.1109/TAC.1974.1100705

31. G. Schwarz, Estimating the dimension of a model, *Ann. Statist.*, **6** (1978), 461–464. https://doi.org/10.1214/aos/1176344136

32. S. Bashir, B. Masood, I. Shahzadi, Z. Al-Husseini, M. Aslam, Neutrosophic Lindley distribution: simulation, application, and comparative study, *Contemp. Math.*, **6** (2025), 551–564. https://doi.org/10.37256/cm.6120256127

33. F. S. Alduais, A neutrosophic extension of the inverse gamma distribution: properties and applications, *Neutrosophic Sets and Systems*, **91** (2025), 423–437.

34. Z. Khan, M. M. Almazah, O. H. Odhah, H. M. Alshanbari, Generalized pareto model: properties and applications in neutrosophic data modeling, *Math. Probl. Eng.*, **2022** (2022), 368696. https://doi.org/10.1155/2022/3686968

AIMS Press